Title
Pregnancy Augments VEGF-Stimulated In Vitro Angiogenesis and Vasodilator (NO and H2S) Production in Human Uterine Artery Endothelial Cells.

Journal
The Journal of Clinical Endocrinology & Metabolism, 102(7)

ISSN
0021-972X

Authors
Zhang, Hong-Hai
Chen, Jennifer C
Sheibani, Lili
et al.

Publication Date
2017-07-01

DOI
10.1210/jc.2017-00437

Peer reviewed

Pregnancy Augments VEGF-Stimulated *In Vitro* Angiogenesis and Vasodilator (NO and H_2S) Production in Human Uterine Artery Endothelial Cells

Hong-hai Zhang,[1] Jennifer C. Chen,[1] Lili Sheibani,[1] Thomas J. Lechuga,[1] and Dong-bao Chen[1]

[1]Department of Obstetrics & Gynecology, University of California, Irvine, California 92697

Context: Augmented uterine artery (UA) production of vasodilators, including nitric oxide (NO) and hydrogen sulfide (H_2S), has been implicated in pregnancy-associated and agonist-stimulated rise in uterine blood flow that is rate-limiting to pregnancy health.

Objective: Developing a human UA endothelial cell (hUAEC) culture model from main UAs of nonpregnant (NP) and pregnant (P) women for testing a hypothesis that pregnancy augments endothelial NO and H_2S production and endothelial reactivity to vascular endothelial growth factor (VEGF).

Design: Main UAs from NP and P women were used for developing hUAEC culture models. Comparisons were made between NP- and P-hUAECs in *in vitro* angiogenesis, activation of cell signaling, expression of endothelial NO synthase (eNOS) and H_2S-producing enzymes cystathionine β-synthase (CBS) and cystathionine γ-lyase, and NO/H_2S production upon VEGF stimulation.

Results: NP- and P-hUAECs displayed a typical cobblestone-like shape in culture and acetylated low-density lipoprotein uptake, stained positively for endothelial and negatively for smooth muscle markers, maintained key signaling proteins during passage, and had statistically significant greater eNOS and CBS proteins in P- *vs* NP-hUAECs. Treatment with VEGF stimulated *in vitro* angiogenesis and eNOS protein and NO production only in P-hUEACs and more robust cell signaling in P- *vs* NP-hUAECs. VEGF stimulated CBS protein expression, accounting for VEGF-stimulated H_2S production in hUAECs.

Conclusion: Comparisons between NP- and P-hUAECs reveal that pregnancy augments VEGF-stimulated *in vitro* angiogenesis and NO/H_2S production in hUAECs, showing that the newly established hUAEC model provides a critical *in vitro* tool for understanding human uterine hemodynamics. (***J Clin Endocrinol Metab* 102: 2382–2393, 2017**)

During pregnancy in eutherian mammals, including humans, the mother's body must make a series of changes to accommodate the growing metabolic demands of the fast-developing fetus (1). Notably, the mother's cardiovascular system makes a number of adaptive changes, including increased blood volume and

ISSN Print 0021-972X ISSN Online 1945-7197
Printed in USA

Received 15 February 2017. Accepted 3 April 2017.
First Published Online 7 April 2017

Abbreviations: AKT, *v-Akt* murine thymoma viral oncogene homolog 1; BCA, β-cyano-L-alanine; BSA, bovine serum albumin; CBS, cystathionine β-synthase; CCD, charge-coupled device; CD31/PECAM1, platelet endothelial cell adhesion molecule 1; CHH, *O*-(carboxymethyl)hydroxylamine hemihydrochloride; CSE, cystathionine γ-lyase; DAF, 4,5-diaminofluorescein; DAF-FM, 4,5-diaminofluorescein diacetate; Dil-Ac-LDL, 1,1-dioctadecyl-3,3,33-tetramethylindocarbocyanine perchlorate–labeled acetylated low-density lipoprotein; EC, endothelial cell; ECM, endothelial cell culture medium; eNOS, endothelial nitric oxide synthase; ERK1/2, extracellular signaling kinases 1/2; FBS, fetal bovine serum; FCS, fetal calf serum; Flt1, fms-related tyrosine kinase 1; H_2S, hydrogen sulfide; hUAEC, human uterine artery endothelial cell; hUASMC, human umbilical artery smooth muscle cell; IgG, immunoglobulin G; KDR, kinase insert domain receptor; NO, nitric oxide; NP, nonpregnant; oUAEC, ovine uterine artery endothelial cell; P, pregnant; P0, passage 0; P1, passage 1; P5, passage 5; PBS, phosphate-buffered saline; SM, smooth muscle; SMA, smooth muscle actin; SMC, smooth muscle cell; UA, uterine artery; UBF, uterine blood flow; VEGF, vascular endothelial growth factor; VEGFR, vascular endothelial growth factor receptor; vWF, von Willebrand factor.

cardiac output, systemic vasodilation, and decreased vascular resistance with no change or slight decrease in blood pressure (2–4). These changes force a redistribution of cardiac output to reproductive organs, especially the uterus, such that a substantially increased volume of blood is delivered to the maternal-fetal interface. For instance, in nonpregnant (NP) ewes, less than 1% to 2% of cardiac output is distributed to the reproductive organs, and this number increases to ~15% to 20% in late pregnant (P) ewes, with the largest portion (>95%) directed to the rapidly developing uteroplacental vascular bed, as reflected by a striking rise in uterine blood flow (UBF) from ~10 mL/min to as high as ~500 to 800 mL/min in NP *vs* P ewes (3). The rise in UBF facilitates the bidirectional maternal-fetal exchange of gases (*i.e.*, O_2 and CO_2) and is the sole provider of nutrients to support fetal and placental growth; this makes UBF a critical rate-limiting factor for pregnancy health. Constrained UBF results in intrauterine growth restriction, preeclampsia, and other pregnancy disorders (1, 5), as well as long-term effects in the mother and newborns (6).

Although the exact mechanisms underlying the pregnancy-associated rise in UBF remain poorly understood, compelling evidence shows that orchestrated networks of vasodilators, including prostacyclin (7), nitric oxide (NO) (8), and vascular endothelial growth factor (VEGF) (9), are significantly augmented locally in the uterine artery (UA). Among them, endothelium NO production via endothelial NO synthase (eNOS) appears to function as a focal mediator as it interacts with nearly all known vasodilators, including estrogens and VEGF (8–10). Our recent work first adds to the mix hydrogen sulfide (H_2S) as a new (to our knowledge) UA vasodilator because H_2S production and the expression of its primary synthesizing enzyme, cystathionine β-synthase (CBS) but not cystathionine γ-lyase (CSE), are significantly stimulated by exogenous estrogens in ovine UA (11) and also are significantly augmented and positively linked to endogenous estrogens in human UA (12). Previous studies show that pregnancy augments endothelium/NO-dependent human UA dilator responses to acetylcholine (13, 14) and enhances VEGF-stimulated relaxation of phenylephrine-constricted rat UA (9). VEGF functions via its specific tyrosine kinase receptors—that is, fms-related tyrosine kinase 1 (Flt1)/VEGR receptor (VEGFR) 1 and kinase insert domain receptor (KDR)/VEGFR2—to activate extracellular signaling kinases 1/2 (ERK1/2) and protein kinase B/*v-Akt* murine thymoma viral oncogene homolog 1 (AKT), which directly phosphorylate and activate eNOS to increase NO production (15, 16). VEGF also stimulates endothelial H_2S production during *in vitro* and *in vivo* angiogenesis (17). Thus, enhanced endothelial NO and H_2S production may contribute to the augmented vascular reactivity to VEGF during pregnancy.

Endothelial cells (ECs), the inner lining of blood vessels, produce nearly all known vasodilators and thus play a central role in hemodynamic regulation. *In vitro* EC cultures are important models for studying the role of endothelium in vascular health. ECs have a common topography throughout the vascular tree; however, significant fundamental differences exist in ECs derived from different vascular beds and organs among different species (18). Thus, the ideal culture model for studying the biology of ECs in a given tissue should be primary ECs from that tissue. Currently, an ovine UA endothelial cell (oUAEC) culture model is the only available cell model that has been exclusively used for studying EC/NO-dependent cellular and molecular mechanisms underlying pregnancy-associated and agonist-stimulated uterine vasodilation (16, 19). It is debatable if the oUAEC data can be translated into human clinical settings due to remarkable species variations in uterine hemodynamics (20). Thus, a primary human UAEC (hUAEC) model is needed for investigating the cellular and molecular mechanisms underlying pregnancy-augmented and agonist-stimulated UA vasodilation in human clinical settings.

The objective of this study was to develop a hUAEC culture model using human main UAs collected from NP and P women for testing a hypothesis that pregnancy augments endothelial NO and H_2S production and endothelial reactivity in response to VEGF stimulation. We report herein for the first time, to our knowledge, successful development of new hUAEC models from NP and P women. Comparisons between NP- and P-hUAECs revealed that not only do significant differences exist in baseline NO and H_2S biosynthesis in NP- *vs* P-hUAECs, but also the differences resemble those observed under *in vivo* conditions, which were retained in culture through passages. Moreover, pregnancy significantly augmented VEGF-stimulated *in vitro* angiogenesis and vasodilator (*i.e.*, NO and H_2S) production in hUAECs.

Materials and Methods

Chemicals and antibodies

Endothelial cell culture medium (ECM) and fetal bovine serum (FBS) were purchased from ScienCell (Carlsbad, CA). Collagenase II was from Life Technologies (Grand Island, NY). 1,1-Dioctadecyl-3,3,33-tetramethylindocarbocyanine perchlorate–labeled acetylated low-density lipoprotein (Dil-Ac-LDL) was from Molecular Probes (Portland, OR). Antibodies against eNOS and CSE were from Santa Cruz Biotechnology (Dallas, TX), KDR and Flt1 were from R&D Systems (Minneapolis, MN), and β-actin was from Ambion (Austin, TX). Monoclonal antibodies against CBS and von Willebrand factor

(vWF) were purchased from Abcam (Cambridge, MA). Antibodies against AKT, ERK1/2, phosphorylated eNOS, phosphorylated AKT, and phosphorylated ERK1/2 were from Cell Signaling Technology (Beverly, MA). Horseradish peroxidase–conjugated goat anti-mouse and anti-rabbit immunoglobulins G (IgGs) were purchased from Thermo Scientific (Waltham, MA). Growth factor–reduced Matrigel matrix was purchased from BD Biosciences (Bedford, MA). Anti–platelet endothelial cell adhesion molecule 1 (CD31/PECAM1) antibody was from Dako (Carpinteria, CA). Prolong Gold antifade reagent with 4′,6-diamidino-2-phenylindole, Alexa 488– and Alexa 568–conjugated goat anti-mouse IgGs, and 4,5-diaminofluorescein (DAF) diacetate (DAF-FM) were from Invitrogen (Carlsbad, CA). β-Cyano-L-alanine (BCA), an inhibitor of CSE, came from Cayman Chemical (Ann Arbor, MI). O-(carboxymethyl)hydroxylamine hemihydrochloride (CHH), an inhibitor of CBS, and all other chemicals unless specified were from Sigma (St. Louis, MO).

Tissue collection

The main UAs were obtained from NP and P women (n = 5/group) in the event of hysterectomy at the University of California Irvine Medical Center. Written consent was obtained from all participants, and ethical approval (HS 2013-9763) was granted by the Institutional Review Board for Human Research at the University of California Irvine. All NP subjects were not taking hormone replacement therapy at the time of tissue collection, were aged 35 to 50 years, and were undergoing elective hysterectomy due to fibroids; they were in the proliferative phases of the menstrual cycle as determined by the last menstrual period recorded and confirmed with endometrial histology. Pregnant subjects were recruited with suspected placental accreta based on previous ultrasound findings in the event a hysterectomy was indicated. They were aged 35 to 44 years and at 35 to 36 weeks' gestation. Both main UAs were dissected from parametrium and paracervical tissues and adjacent myometrium, placed in chilled ECM, and transported to the laboratory.

Cell isolation, purification, culture, and characterization

UAs were dissected free of connective tissues and rinsed free of blood by phosphate-buffered saline (PBS). After gently flushing with PBS, intact UA segments (normally ~4 cm long) were filled with PBS containing 2 mg/mL collagenase II with one end tightened. After tightening the other end, the UAs were placed in a moisture dish and allowed for digestion at 37°C for 45 minutes. EC sheets were flushed out with 1 mL ECM. The flushing was plated in a 100-mm culture dish with a total volume of 10 mL complete ECM with 5% fetal calf serum (FCS) and 1% antibiotics. Following 5 days in culture, EC colonies were manually picked up by a small filter paper soaked with 0.25% trypsin-EDTA. The colonies were individually plated into wells of a 24-well plate; after 7 days in culture, the cells in each well were transferred into a 100-mm dish. After another 7 days in culture, the cells were designed as passage 1 (P1) and stored in liquid N_2. Both NP- and P-hUAECs at P1 were thawed and cultured in ECM/5% FCS and 1% antibiotics in a 100-mm dish to ~70% confluence and subcultured up to passage 5 (P5) for experimental use.

A tube-shaped large artery like the main UAs contained the luminal surface intima of a thin layer of ECs and the media composed of a thick layer of smooth muscle cells (SMCs). We also observed human umbilical artery smooth muscle cell (hUASMC) colonies in the passage 0 (P0) culture. The hUASMC colonies were picked up manually with trypsin-soaked filter papers and plated in a 24-well plate and cultured in Dulbecco's modified Eagle medium/5% FBS and antibiotics. After 7 days in culture, the cells in each well were transferred into a 100-mm dish. After 7 days in culture, the cells were designed as P1 and stored in liquid N_2. hUASMCs at P1 were thawed and cultured in 5% Dulbecco's modified Eagle medium/5% FCS and 1% antibiotics in a 100-mm dish to reach ~70% confluency and subcultured up to P5 for experimental use. Both hUAECs and hUASMCs were characterized by morphology in culture using phase-contrast light microscopy, Dil-Ac-LDL uptake, immunofluorescence microscopy, and immunoblotting of EC *vs* smooth muscle (SM) marker proteins.

Dil-Ac-LDL uptake

Cells were seeded in a collagen-coated 6-well plate. After reaching ~70% confluence, the cultures were washed once with culture medium and then incubated with fresh medium containing 10 μg/mL Dil-Ac-LDL and cultured at 37°C for 4 hours. The cultures were washed three times with fresh medium and cultured for 16 hours. The cells were examined under an inverted Leica fluorescence microscopy (Leica Corp., Deerfield, IL) for image acquisition and captured by a Hamamatsu (Bridgewater, NJ) charge-coupled device (CCD) camera using the *Simple*PCI image analysis software.

Immunofluorescence microscopy

Cells were cultured on collagen-coated glass coverslips. After being washed with cold PBS, the cells were fixed with 4% paraformaldehyde. Nonspecific binding was blocked with PBS containing 1% gelatin, 1% bovine serum albumin (BSA), and 0.15% saponin for 20 minutes. The cells were then incubated with mouse monoclonal antibodies against human CD31 (1 μg/mL), anti-vWF (1 μg/mL), and α–smooth muscle actin (α-SMA, 1 μg/mL) in PBS containing 0.5% gelatin, 0.5% BSA, and 0.075% saponin for 1 hour. After washing with the same buffer three times, the cells were incubated with Alexa 488 goat anti-mouse IgG (1 μg/mL) for anti-CD31 and anti-vWF or Alexa 568 goat anti-mouse IgG for α-SMA, respectively, at room temperature for 1 hour. The cells were mounted in Prolong Gold antifade reagent with 4′,6-diamidino-2-phenylindole and examined under an inverted Leica fluorescence microscope for image acquisition by a Hamamatsu CCD camera with *Simple*PCI.

In vitro angiogenesis assays

Mitogenesis

Cell proliferation was determined by using the xCELLigence system (Roche Diagnostics, Quebec City, Quebec, Canada). The xCelligence is a microelectronic biosensor system for cell-based assays for monitoring cell proliferation, adhesion, and migration by quantifying cell impedance in a real-time and dynamic manner (21). Cells (1×10^4 cells/well) were seeded in quadruplicate with 200 μL M199 0.1% BSA and 25 mM HEPES into an E-plate 16 specifically designed to measure cellular impedance (Roche Diagnostics) and cultured overnight. The impedance of cells was captured every 5 minutes up to 24 hours in culture. The impedance value was expressed as an

arbitrary unit called the cell index, which reflects changes in cell proliferation.

Cell migration

Cell migration was determined by using a scratch "wound" assay (22), with minor modifications. Briefly, hUAECs were grown on collagen-coated 6-well plates. A confluent hUAEC monolayer was scrapped by using a sterilized 200-μL pipette tip. After wounding, the cells were washed with serum-free M199 and cultured in M199 containing 0.1% BSA and 0.5% FCS with or without VEGF for 24 hours. The distance of the cells moved from the wounding edge toward the center of the wound was measured and averaged as an index for cell migration.

Tube formation

Growth factor–reduced Matrigel was applied to a 48-well plate and allowed to polymerize at 37°C for 30 minutes. hUAECs were resuspended in M199 0.1% BSA and 25 mM HEPES. Cells (1×10^5 cells) were seeded into each well in a 500-μL volume and incubated under 5% CO_2 in air at 37°C. Treatments were added at the beginning of incubation. After a 4-hour incubation, tube formation was assessed under an inverted Leica microscopy with ×10 objectives. Digitalized bright-field images were captured by a Hamamatsu CCD camera using *Simple*PCI. Images of three randomly chosen fields of each well were captured. The branch points of the formed tube-like structures were quantified and averaged.

Cell stimulation, sodium dodecyl sulfate polyacrylamide gel electrophoresis, and immunoblotting

NP- and P-hUAECs at passage 4 to P5 were treated without or with VEGF (10 ng/mL). Cellular proteins were harvested in a nondenaturing buffer (16). Proteins (20 μg/lane) were separated on 8% to 10% sodium dodecyl sulfate polyacrylamide gel electrophoresis and transferred onto polyvinylidene difluoride membranes and immunoblotted as described previously (23). Proteins of interest were measured by immunoblotting with antibodies against eNOS (0.5 μg/mL), CBS (5 μg/mL), CSE (1 μg/mL), Flt1 (2 μg/mL), KDR (2 μg/mL), Akt (1 μg/mL), ERK1/2 (1 μg/mL), phosphorylated NOS^{1177} (1 μg/mL), phosphorylated Akt (1 μg/mL), phosphorylated ERK1/2 (0.5 μg/mL), and β-actin (0.2 μg/mL). Quantification of band intensity was performed using NIH ImageJ 1.60 (National Institutes of Health, Bethesda, MD).

DAF-FM fluorescence for NO determination

hUAECs were plated on a glass coverslip–bottomed 6-well plate and loaded with 2 μM DAF-FM diacetate for 30 minutes in Dulbecco's PBS with Ca^{2+} and Mg^{2+} supplemented with glucose (1 mg/mL) and L-arginine (1 mM). Cells were then washed three times with Dulbecco's PBS to remove excess probe. The cells were incubated at 37°C for another 30 minutes to allow de-esterification of the probe to form the cell-impermeable DAF-FM. After treatment, DAF-FM–loaded cells in dishes were placed on the stage of an inverted Leica fluorescence microscope for fluorescence image acquisition by a Hamamatsu CCD camera with ×20 fluor objectives (Zeiss, New York, NY) using *Simple*PCI. Digitalized images (three per well per treatment) were captured. Intracellular NO production was quantified by averaging the relative fluorescence intensity of 10 cells per image of the three images per treatment.

Methylene blue assay

Cells (5×10^5/treatment in duplicate) were homogenized in ice-cold 50 mM potassium phosphate buffer, pH 8. H_2S production was determined by the methylene blue assay as previously described (11, 12). H_2S concentration was calculated based on a calibration curve generated from sodium hydrosulfide (NaHS) solutions. For CBS and CSE inhibition experiments, their respective inhibitor CHH or BCA was added separately or in combination (final concentration = 2 mM) to the reaction mixtures prior to initiating the assay.

Experimental replication and statistical analysis

All experiments were repeated at least three times using cells from different subjects. Data were presented as mean ± standard deviation and analyzed by one-way analysis of variance, followed by the Student-Newman-Keuls test for multiple comparisons. Significant difference was defined as $P < 0.05$.

Results

Characterization of hUAECs and hUASMCs

hUAECs exhibited classic cobblestone EC morphology and were maintained in a monolayer that did not overgrow after reaching confluence throughout five passages, whereas hUASMCs displayed a typical SMC spindlelike shape throughout five passages and grew in a multilayer after reaching confluence [Fig. 1(a) and 1(b)]. All live hUAECs, but not hUASMCs, absorbed Dil-Ac-LDL in culture [Fig. 1(c) and 1(d)]. Both NP- and P-hUAECs stained positively and uniformly with vWF [Fig. 1(e)]. The immunoreactive signals showed rod-shaped structures throughout the cytoplasm, characteristic of the most reliable EC marker, Weibel-Palade bodies (24). All hUAECs stained positively with a highly specific EC marker, CD31 [Fig. 1(g)], but negatively with the specific SM marker, α-SMA [Fig. 1(i)]. In contrast, hUASMCs stained negatively with EC marker vWF or CD31 [Fig. 1(f) and 1(h)] but positively stained with α-SMA and showed filamentous projections [Fig. 1(j)].

Protein expression of vasodilator producing enzymes and VEGFR in P-hUAECs during passage

Only very few primary hUAECs can be obtained from the main UAs of a woman. Thus, it is essential to propagate the cells at P0 by passage so that adequate cells can be obtained with subculture for studying EC-dependent mechanisms of pregnancy-associated and agonist-stimulated uterine vasodilation. To this end, whether the *in vivo* features of hUAECs can be retained during passage is critical for the hUAEC cell model. We examined if levels of proteins of interest, including eNOS,

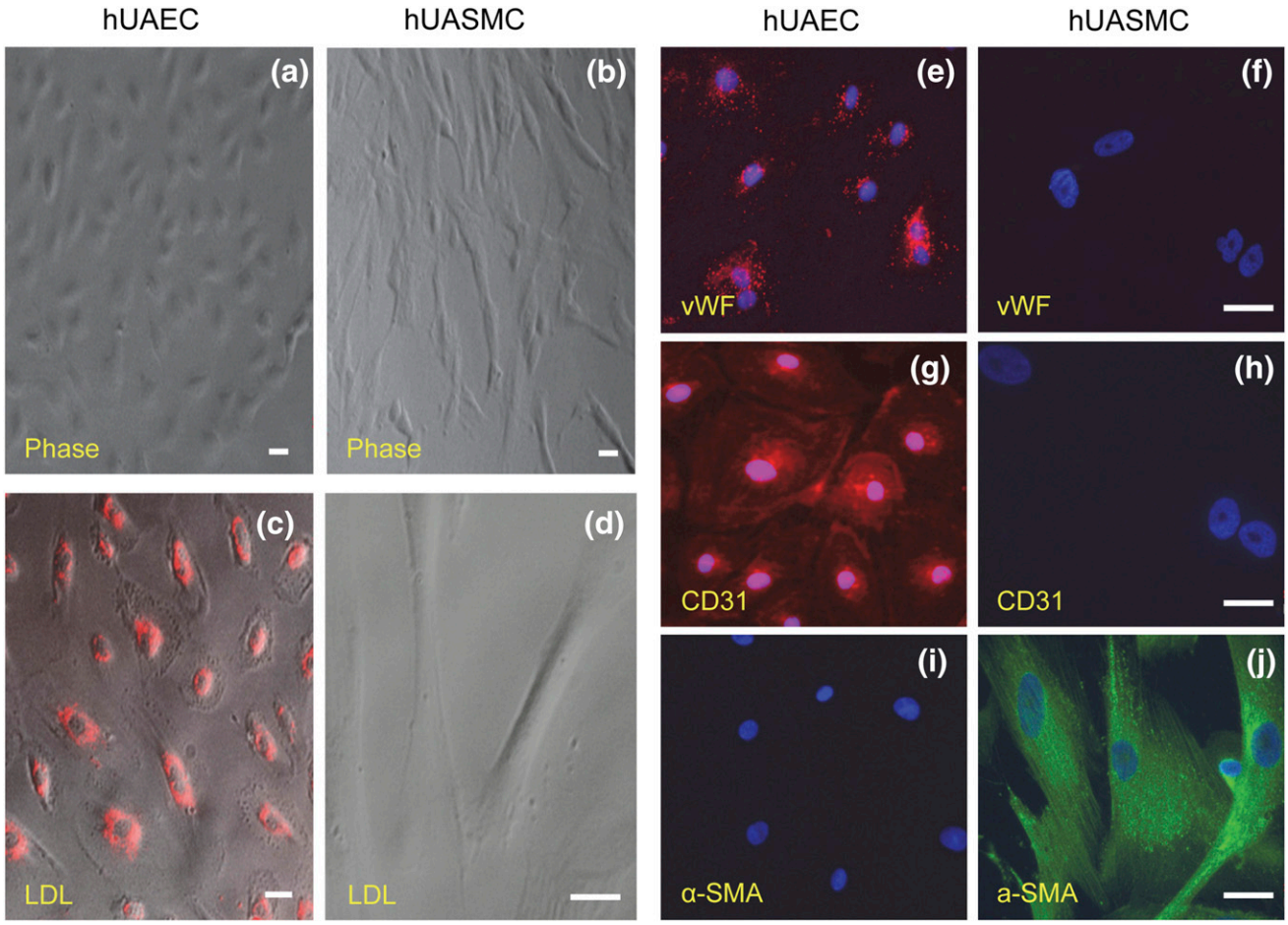

Figure 1. Characteristics of hUAECs and hUASMCs. Both hUAECs and hUASMCs were characterized by morphology in culture using (a, b) phase-contrast light microscopy, (c, d) Dil-Ac-LDL uptake, and immunofluorescence labeling with EC *vs* SM marker proteins, including (e, f) vWF, (g, h) CD31, and (i, j) α-SMA. Scale bar = 20 μm.

CBS, CSE, VEGFR (*i.e.*, KDR and Flt1), and α-SMA, are altered during passage. P-hUAECs expressed all, but not α-SMA, of these proteins during five passages. Levels of eNOS, Flt1, and CBS proteins significantly decreased at passage 2 ($P < 0.05$) and maintained at the passage 2 levels through P5, whereas levels of KDR and CSE proteins were unchanged. P-hUASMCs expressed CBS, CSE, Flt1, and α-SMA, with no detectable eNOS and KDR proteins (Fig. 2).

Pregnancy augments VEGF-stimulated *in vitro* angiogenesis in hUAECs

One important feature of ECs is to respond to angiogenic growth factors to form new blood vessels, a process termed *angiogenesis*. VEGF is, perhaps, the most important growth factor that regulates an array of EC functions, including angiogenesis (25). Treatment with VEGF (10 ng/mL) significantly stimulated cell proliferation, migration, and tube formation in P-hUAECs but not NP-hUAECs. As a control, 5% FBS stimulated cell proliferation, migration, and tube formation in both P- and NP-hUAECs [Fig. 3(a–c)].

Protein expression in NP- *vs* P-hUAECs

When cells are cultured *in vitro*, they reside in a microenvironment completely different from the one they reside *in vivo*. The maintenance of the *in vivo* characteristics of NP- *vs* P-hUAECs is critical for their usage in examining pregnancy-dependent mechanisms. Levels of eNOS and CBS but not CSE proteins were significantly greater in P- *vs* NP-hUAECs in culture (Fig. 4). These findings resemble the reports from us and others showing augmented NO production due to upregulation of eNOS protein (8, 12) and H_2S production due to significant upregulation of EC expression of CBS but not CSE proteins in human umbilical artery *in vivo* (12). In addition, Flt1 protein was significantly greater and KDR was similar in P- *vs* NP-hUAECs.

Pregnancy augments VEGF-stimulated cell signaling and eNOS/NO production in hUAECs

As pregnancy augmentation of VEGF-stimulated UA relaxation is mediated largely by increasing EC NO production *in vivo* (9), presumptively through direct eNOS activation *via* ERK1/2 and Akt-dependent

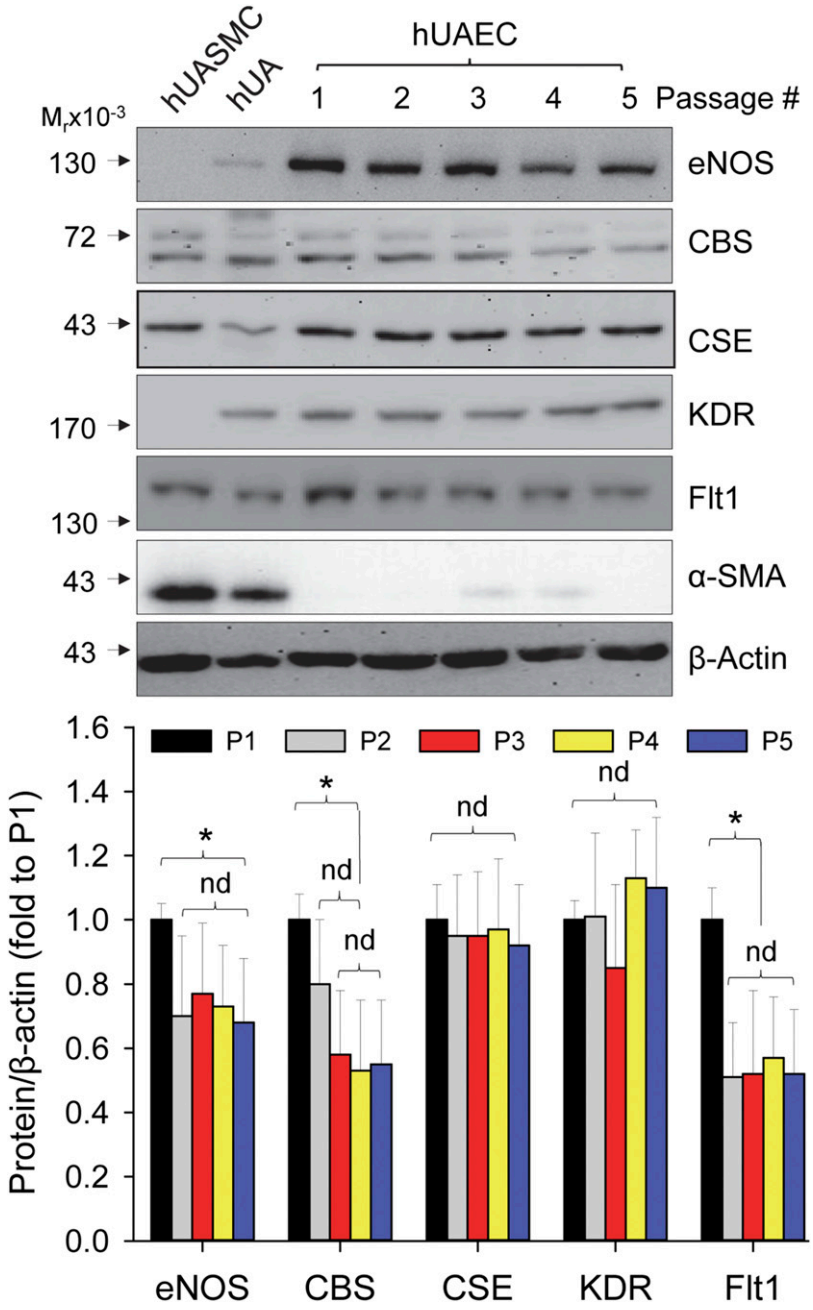

Figure 2. Protein expression during passage in hUAECs. P-hUAECs were passaged five times. Cellular proteins were extracted for analyzing levels of eNOS, CBS, CSE, KDR, Flt1, and α-SMA by immunoblotting with specific antibodies. Lysates from intact human UA and P-UASMCs were used as controls. Images in the upper panels show a typical experiment. Bar graph in lower panel summarizes changes of levels of proteins during five passages. Data (mean ± standard deviation, n = 5) were converted to fold of P1 after normalization to β-actin. *$P <$ 0.05 *vs* P1. nd, no difference.

phosphorylation (15, 16), we determined differences in phosphorylation of eNOS and its activating enzymes ERK1/2 and Akt in P- *vs* NP-hUAECs. Treatment with VEGF (10 ng/mL) for 10 minutes significantly stimulated phosphorylation of ERK1/2, but not eNOS and Akt, in NP-hUAECs, whereas VEGF significantly stimulated phosphorylation of ERK1/2, Akt, and eNOS in P-hUAECs. However, the response of ERK1/2 phosphorylation is more robust in P- *vs* NP-hUAECs [Fig. 5(a)]. Treatment with VEGF (10 ng/mL) for 48 hours significantly stimulated eNOS protein expression in P-hUAECs but not NP-hUAECs [Fig. 5(b)]. Treatment with VEGF (10 ng/mL) also rapidly stimulated time-dependent NO production, as determined by DAF-AM fluorescence imaging, in P-hUAECs but not NP-hUAECs. NO production in P-hUAECs increased at 2 minutes and continued to rise at 5 to 10 minutes after treatment with VEGF [Fig. 5(c)].

Pregnancy augments VEGF-stimulated CBS expression and H_2S production in hUAECs

We then examined the effects of VEGF on CBS and CSE protein expression and H_2S production in NP- *vs* P-hUAECs to determine whether VEGF stimulates hUAEC H_2S production and whether this is augmented by pregnancy. Treatment with VEGF (10 ng/mL) for 48 hours significantly stimulated CBS protein expression in P-hUAECs but not NP-hUAECs [Fig. 6(a)]. Baseline H_2S production (25.35 ± 0.89 nM/μg protein/h, n = 3) in P-hUAECs was significantly greater than that (8.85 ± 0.28 nM/μg protein/h, n = 3) in NP-hUAECs ($P < 0.001$). Treatment with VEGF (10 ng/mL) for 48 hours stimulated H_2S production in both P- and NP-hUAECs ($P < 0.001$). Co-incubation with a specific CBS inhibitor, CHH, significantly lowered baseline H_2S production in both P- and NP-hUAECs; it completely abolished VEGF-stimulated H_2S production and further lowered the levels to baseline co-incubated with CHH in both P- and NP-hUAECs. In contrast, co-incubation with a specific CSE inhibitor, BCA, had no effect on baseline and VEGF-stimulated H_2S production in both P- and NP-hUAECs. The combination of CHH and BCA had no additive effects on H_2S production in both P- and NP-hUAECs [Fig. 6(b) and 6(c)].

Discussion

We report herein successful development of what we believe is a new hUAEC cell culture model from main UAs

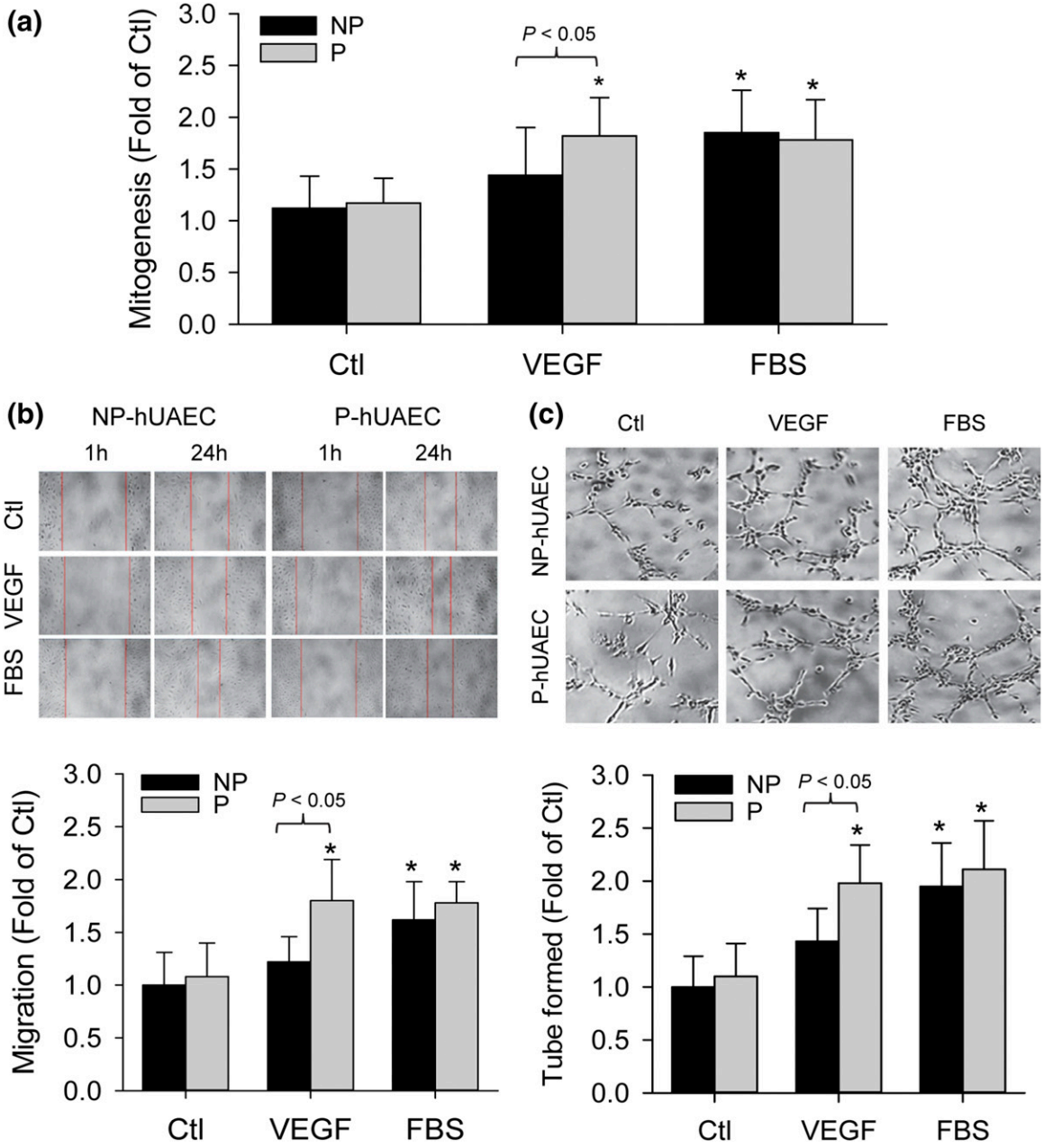

Figure 3. Pregnancy augments VEGF-stimulated *in vitro* angiogenesis in hUAECs. Both NP- and P-hUAECs at passages 4 to 5 were treated with or without VEGF (10 ng/mL) or 5% FBS and subjected to assays for cell proliferation by using the (a) xCELLigence system, (b) migration by using a scratch wound assay, and (c) tube formation on Matrigel. Bar graphs shown summarize data (mean ± standard deviation, n = 3) using cells derived from three different NP and P women. *$P < 0.05$ *vs* NP control. Ctl, control.

of both P and NP women. There are significant differences in baseline expression of vasodilator (*i.e.*, NO and H_2S) producing enzymes, including eNOS, CBS, CSE, and VEGFRs, in P- *vs* NP-hUAECs, which are maintained during passage. With these cell models, we show that VEGF significantly stimulates *in vitro* angiogenesis in P-hUAECs but not NP-hUAECs. VEGF also significantly stimulates activation of the eNOS-NO pathway (*i.e.*, ERK1/2 and Akt activation, eNOS phosphorylation, and NO production), consistent with previous findings with oUAECs (19). Moreover, we report for the first time, to our knowledge, that VEGF stimulates H_2S production through selective CBS upregulation in P- *vs* NP-hUAECs *in vitro*. Collectively, our data show that pregnancy significantly augments VEGF-stimulated *in vitro* angiogenesis and vasodilator (NO and H_2S) production in hUAECs.

A hUAEC cell culture model has long been sought after. However, the development of such a model has been hindered by technical difficulties due to the unique structural features of human UA, which contains the luminal surface intima composed of a thin layer of ECs

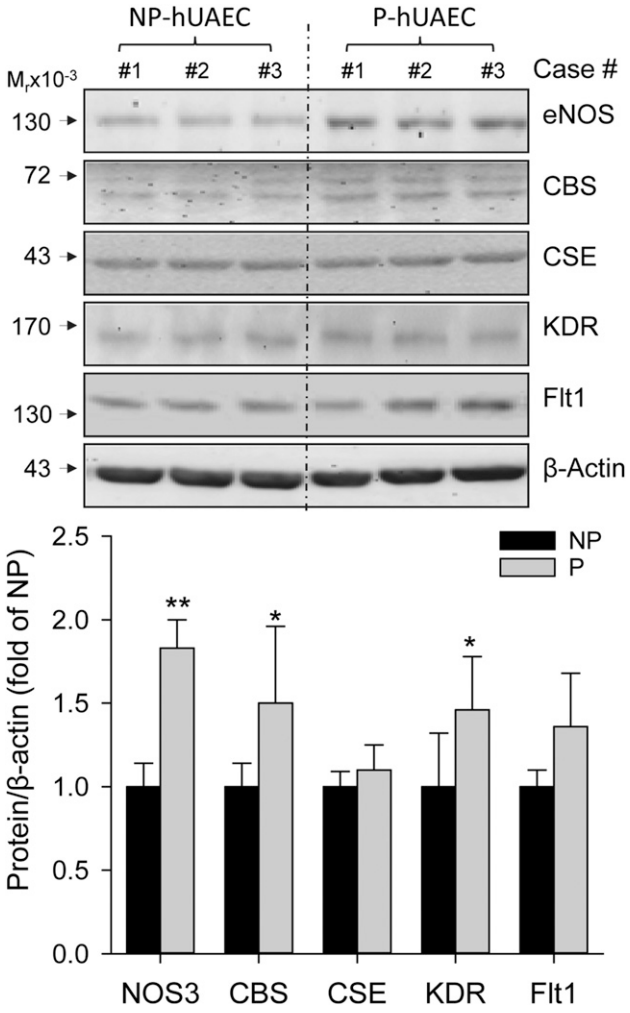

Figure 4. Pregnancy-dependent expressions of proteins in hUAECs. Protein samples were extracted from both NP- and P-hUAECs at passages 4 to 5. Proteins (20 μg/lane) were used for analyzing levels of eNOS, CBS, CSE, KDR, Flt1, and β-actin proteins by immunoblotting with specific antibodies. Images shown in upper panel represent blots of a typical experiment. Bar graph in lower panel summarizes data (mean ± standard deviation, n = 3) calculated as fold of baseline in NP-hUAECs after normalization with β-actin. $*P < 0.05$ and $**P < 0.01$ *vs* NP.

and the media composed of a thick layer of SMCs. In many attempts by using the most common technique with collagenase digestion for development of the oUAEC model (19), we have noticed that the isolated primary hUAEC cultures are always contaminated by undesired SMCs and pericytes. In the impure P0 cultures, the progressive increase in the number of SMCs and/or pericytes results in arrest of EC proliferation, as previously reported (26). Thus, additional purification steps are needed to achieve homogeneous cultures. Although cell sorting is commonly used to purify specific EC types, this procedure shortens the life span of ECs (27). Therefore, we have chosen to use a manual colony pickup technique for purifying hUAECs. Although this procedure is tedious and time-consuming, the purity of hUAEC colonies picked up ensures that the established hUAEC model has a uniform EC identity (Figs. 1 and 2). Another advantage of the manual pickup purification technique is that a novel hUASMC model was established from the same P0 culture derived from the same UA donor. The paired hUAECs and hUASMCs models from the same UA donor offer unique opportunities for studying EC *vs* SM mechanisms of uterine vasodilation.

Because ECs possess considerable phenotypic heterogeneity (28, 29), we have used a combination of endothelial characteristics to determine the identity and purity of our cultures. We provide several lines of evidence showing that our hUAEC model is homogeneous EC in origin, including uniform cobblestone EC morphology in culture throughout five passages, rapid DiI-Ac-LDL uptake, and positive staining of EC-specific markers CD31 and vWF and negative staining of the SMC-specific marker α-SMA. CD31 is considered one of the most reliable EC markers, which is not expressed in SMCs, pericytes, and fibroblasts (25, 30). The vWF-related antigen is expressed at significantly high levels only in certain cells, including ECs, megakaryocytes, and human syncytiotrophoblasts; the latter two are impossible to be present in our cells. vWF is associated with the EC-specific granules called Weibel-Palade bodies (24), consistent with the staining pattern in hUAECs. Moreover, hUAECs are maintained in a monolayer and do not overgrow, even when reaching 100% confluence during passage, displaying an EC-typical growth pattern (31); this feature also shows that our cells are devoid of SMCs, pericytes, and fibroblasts that tend to grow in multiple layers, which is further supported by negative expression of the SM-specific marker α-SMA.

ECs proliferate, migrate, and differentiate to form new tube-like structures, collectively called *in vitro* angiogenesis (25). Our hUAECs from both P and NP women can be induced to proliferate, migrate, and form tube-like structures on Matrigel by a nonspecific angiogenic promoter, 5% FBS *in vitro*. VEGF, perhaps, is the most important growth factor that regulates an array of the functions of ECs, including angiogenesis (25). However, VEGF induces angiogenesis *in vitro* only in P-hUAECs but not NP-hUAECs. These data show that pregnancy augments VEGF-stimulated angiogenesis in hUAECs.

ECs in blood vessels of all sizes express eNOS (32). Our current data show that both P- and NP-hUAECs express high-level eNOS protein that is maintained during passages. Enhanced EC NO production *via* increased expression and/or activation of eNOS protein is an essential signaling molecule critical for vascular health, participating in the regulation of numerous physiological and pathological processes. Previous studies have shown that pregnancy augments the expression and activity of

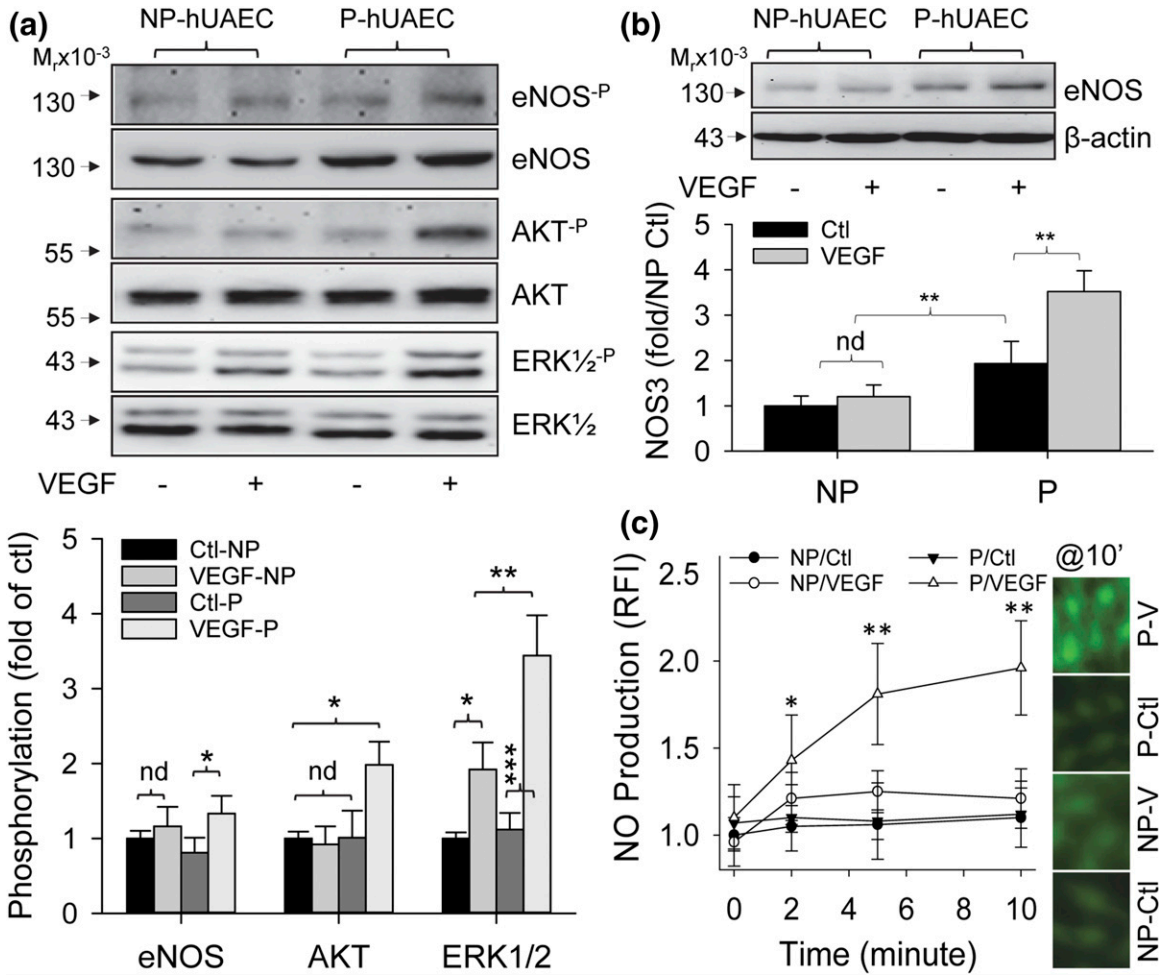

Figure 5. Pregnancy augments VEGF-stimulated eNOS expression/activation and NO production in hUAECs. (a) Both NP- and P-hUAECs at passages 4 to 5 were treated with or without VEGF (10 ng/mL) for 10 minutes. Proteins were collected for analyzing phosphorylation of eNOS, AKT, and ERK1/2 by immunoblotting with specific antibodies. Phosphorylation was determined by a ratio between phosphorylated *vs* total protein. Images shown in upper panel represent blots from a typical experiment. Bar graph in lower panel summarizes data (mean ± standard deviation, n = 3) calculated as fold of NP-hUAECs after normalization with β-actin. $^{*}P < 0.05$, $^{**}P < 0.01$, $^{***}P < 0.001$. Ctl, control; nd, no difference. (b) Both NP- and P-hUAECs at passages 4 to 5 were treated with or without VEGF (10 ng/mL) for 48 hours. Proteins were collected for analyzing eNOS and β-actin proteins by immunoblotting with specific antibodies. Images shown in upper panel represent blots from a typical experiment. Bar graph in lower panel summarizes data (mean ± standard deviation, n = 3) calculated as fold of NP-hUAECs after normalization with β-actin. $^{**}P < 0.01$. (c) Both NP- and P-hUAECs at passages 4 to 5 were grown in glass coverslip–bottomed dishes. After being loaded with DAF-FM, the cells were treated with or without VEGF (10 ng/mL) for determining intracellular NO production for up to 10 minutes. Levels of intracellular NO were quantified by relative fluorescence intensity (RFI) and calculated as fold of time zero. Images shown on right represent fluorescence images at 10 minutes of a typical experiment. Bar graph on left summarizes data (mean ± standard deviation, n = 3) calculated as fold of time zero. $^{*}P < 0.05$ and $^{**}P < 0.01$ *vs* time zero.

eNOS and NO production in human UA (14), and pregnancy significantly augments endothelium/NO-dependent human UA dilator responses to acetylcholine (13). Enhanced NO production *via* eNOS is well-known to play a critical role in mediating EC proliferation and migration during angiogenesis upon VEGF stimulation (17, 22, 33). Animal studies also have shown that pregnancy potentiates VEGF-stimulated relaxation of phenylephrine-constricted rat UA, in part by endothelium/NO-dependent mechanisms (9, 34). These reports show that endothelial NO production is important for pregnancy-augmented and agonist-stimulated uterine vasodilation. We have shown herein that VEGF rapidly stimulates phosphorylation of ERK1/2 and Akt, two upstream activators of eNOS (15, 16), in hUAECs but with more robust responses in the P *vs* NP state, which may be responsible for rapid VEGF-stimulated eNOS phosphorylation in P-hUAECs but not NP-hUAECs. VEGF also stimulates rapid NO production in P-hUAECs but not NP-hUAECs, consistent with VEGF stimulation of eNOS protein expression in P-hUAECs but not NP-hUAECs. Thus, pregnancy augments the VEGF-stimulated endothelial eNOS-NO pathway *via* increasing eNOS expression and its activation in hUAECs *in vitro*.

Endogenous H_2S is mainly synthesized by two key enzymes, CBS and CSE, and these enzymes produce H_2S

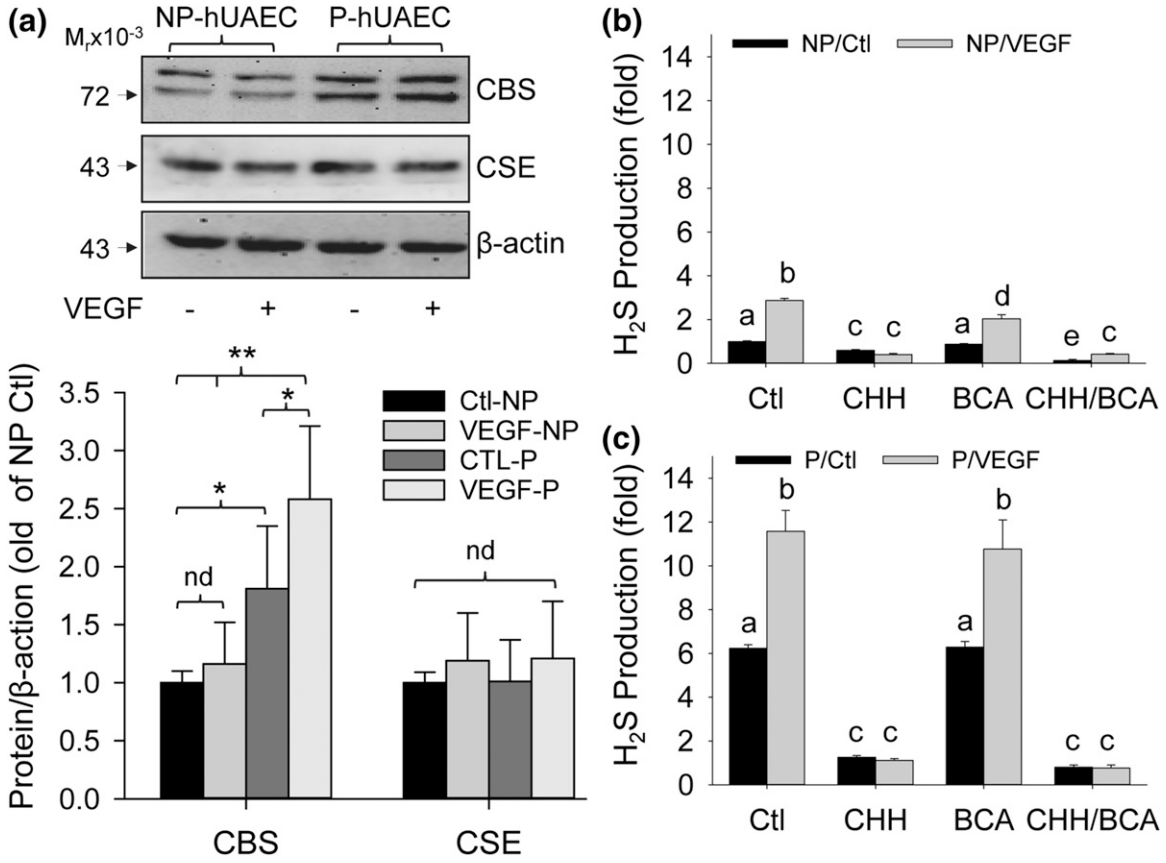

Figure 6. Pregnancy augments VEGF-stimulated H_2S biosynthesis in hUAECs. Both NP- and P-hUAECs at passages 4 to 5 were treated with or without VEGF (10 ng/mL) for 48 hours. Proteins were collected for analyzing CBS, CSE, and β-actin proteins by immunoblotting with specific antibodies and H_2S production in NP- *vs* P-hUAECs in the presence of inhibitors of CBS (CHH), CSE (BCA), or both by the methylene blue assay. (a) Upper panel: blots from a typical experiment. Lower panel: bar graph summarizes data (mean ± standard deviation, n = 3) calculated as fold of NP-hUAECs after normalization with β-actin. $^*P < 0.05$, $^{**}P < 0.01$. nd, no difference. (b, c) Bar graphs summarizes data (mean ± standard deviation, n = 3) calculated as fold of baseline in NP-hUEACs. Bars with different letters differ significantly ($P < 0.05$).

from L-cysteine, CBS via a β-replacement reaction with a variety of thiols and CSE by disulfide elimination followed by reaction with various thiols (35). In mammals, H_2S potently dilates various vascular beds *via* an activating adenosine triphosphate–dependent potassium (K_{ATP}) channel (36) and relaxes smooth muscle via activating a large-conductance calcium-activated potassium (BK_{Ca}) channel (37). H_2S also promotes angiogenesis *in vitro* and *in vivo* (17). Thus, H_2S functions as a potent vasodilator (38). Recent studies have highlighted a role of CSE/H_2S in placental development and function as well as pregnancy because 1) H_2S potently dilates placental vasculature, and 2) dysregulation of CSE expression results in maternal hypertension and placental abnormalities in preeclampsia (39). VEGF stimulates H_2S production in HUVECs *in vitro* and during *in vivo* angiogenesis, primarily involving CSE (17). We have shown that a slow-releasing H_2S donor GYY4137 dilates phenylephrine-preconstricted rat UAs with significantly greater potency in P *vs* NP states, with vascular bed–specific effects (12). Our current data show that VEGF stimulates CBS, but not CSE, protein expression in P-hUAECs but not NP-hUAECs. Unexpectedly, we observed that VEGF stimulates H_2S production in both P- and NP-hUAECs. However, the VEGF-stimulated H_2S production in P- and NP-hUAECs is completely abolished by a specific inhibitor of CBS but not CSE. Although it is not clear why VEGF stimulates H_2S production in NP-UAECs without altering CBS/CSE expression, this is likely related to increased CBS and/or CSE activity due to posttranslational modifications such as binding to Ca^{2+}/calmodulin (38). Nonetheless, pregnancy augments VEGF stimulation of hUAEC H_2S biosynthesis *via* selective CBS upregulation *in vitro*, consistent with our reports that H_2S biosynthesis is significantly augmented in human UA in association with endogenous estrogens during the proliferative phase and pregnancy (12) and in ovine UA (11) by exogenous estrogen stimulation *in vivo*, *via* selective upregulation of EC and SM CBS, but not CSE, messenger RNA/protein.

Altogether, with our established hUAEC models from both NP and P women, we show that not only are there significantly greater baseline expressions of the key enzymes for NO and H_2S production in P- *vs* NP-hUAECs,

but pregnancy also significantly augments VEGF-stimulated *in vitro* angiogenesis and NO/H_2S production in hUAECs *in vitro*. Importantly, these findings consistently resemble the pregnancy-augmented changes in angiogenesis and vasodilator production as seen in human UA *in vivo*. Considering that oUAEC is the only cell model currently available for studying EC-dependent cellular and molecular mechanisms of uterine vasodilation, our hUEAC model provides a critical *in vitro* system for understanding human uterine hemodynamics and its dysregulation.

Acknowledgments

We thank all the participants for donating the tissue samples and the attending physicians of the Department of Obstetrics & Gynecology at the University of California Irvine for their assistance in tissue collection.

Current Affiliation: L. Sheibani's current affiliation is the Department of Obstetrics and Gynecology, University of Southern California, Los Angeles, CA 90033.

Address all correspondence and requests for reprints to: Dong-bao Chen, PhD, Department of Obstetrics and Gynecology, University of California Irvine, Med Surge 1, Bldg 56, Rm 140, Irvine, California 92697. E-mail: dongbaoc@uci.edu.

This work was supported in part by National Institutes of Health (NIH) Grants HL70562, HL98746, and HD84972 (to D.-B.C.). The content is solely the responsibility of the authors and does not necessarily reflect the official views of the NIH.

Disclosure Summary: The authors have nothing to disclose.

References

1. Reynolds LP, Caton JS, Redmer DA, Grazul-Bilska AT, Vonnahme KA, Borowicz PP, Luther JS, Wallace JM, Wu G, Spencer TE. Evidence for altered placental blood flow and vascularity in compromised pregnancies. *J Physiol*. 2006;**572**:51–58.
2. Ramsey EM, Corner GW Jr, Donner MW. Serial and cineradioangiographic visualization of maternal circulation in the primate (hemochorial) placenta. *Am J Obstet Gynecol*. 1963;**86**:213–225.
3. Rosenfeld CR. Distribution of cardiac output in ovine pregnancy. *Am J Physiol*. 1977;**232**:H231–H235.
4. Palmer SK, Zamudio S, Coffin C, Parker S, Stamm E, Moore LG. Quantitative estimation of human uterine artery blood flow and pelvic blood flow redistribution in pregnancy. *Obstet Gynecol*. 1992;**80**:1000–1006.
5. Carr DJ, Wallace JM, Aitken RP, Milne JS, Martin JF, Zachary IC, Peebles DM, David AL. Peri- and postnatal effects of prenatal adenoviral VEGF gene therapy in growth-restricted sheep. *Biol Reprod*. 2016;**94**:142.
6. Barker DJ. Intrauterine programming of adult disease. *Mol Med Today*. 1995;**1**:418–423.
7. Fitzgerald DJ, Entman SS, Mulloy K, FitzGerald GA. Decreased prostacyclin biosynthesis preceding the clinical manifestation of pregnancy-induced hypertension. *Circulation*. 1987;**75**:956–963.
8. Rosenfeld CR, Cox BE, Roy T, Magness RR. Nitric oxide contributes to estrogen-induced vasodilation of the ovine uterine circulation. *J Clin Invest*. 1996;**98**:2158–2166.
9. Ni Y, May V, Braas K, Osol G. Pregnancy augments uteroplacental vascular endothelial growth factor gene expression and vasodilator effects. *Am J Physiol*. 1997;**273**:H938–H944.
10. Zhang HH, Feng L, Wang W, Magness RR, Chen DB. Estrogen-responsive nitroso-proteome in uterine artery endothelial cells: role of endothelial nitric oxide synthase and estrogen receptor-beta. *J Cell Physiol*. 2011;**227**:146–159.
11. Lechuga TJ, Zhang HH, Sheibani L, Karim M, Jia J, Magness RR, Rosenfeld CR, Chen DB. Estrogen replacement therapy in ovariectomized nonpregnant ewes stimulates uterine artery hydrogen sulfide biosynthesis by selectively up-regulating cystathionine beta-synthase expression. *Endocrinology*. 2015;**156**:2288–2298.
12. Sheibani L, Lechuga TJ, Zhang HH, Hameed A, Wing DA, Kumar S, Rosenfeld CR, Chen DB. Augmented H2S production via cystathionine-beta-synthase upregulation plays a role in pregnancy-associated uterine vasodilation. *Biol Reprod*. 2017;**96**:664–672.
13. Nelson SH, Steinsland OS, Suresh MS, Lee NM. Pregnancy augments nitric oxide–dependent dilator response to acetylcholine in the human uterine artery. *Hum Reprod*. 1998;**13**:1361–1367.
14. Nelson SH, Steinsland OS, Wang Y, Yallampalli C, Dong YL, Sanchez JM. Increased nitric oxide synthase activity and expression in the human uterine artery during pregnancy. *Circ Res*. 2000;**87**:406–411.
15. Dimmeler S, Fleming I, Fisslthaler B, Hermann C, Busse R, Zeiher AM. Activation of nitric oxide synthase in endothelial cells by Akt-dependent phosphorylation. *Nature*. 1999;**399**:601–605.
16. Chen DB, Bird IM, Zheng J, Magness RR. Membrane estrogen receptor–dependent extracellular signal–regulated kinase pathway mediates acute activation of endothelial nitric oxide synthase by estrogen in uterine artery endothelial cells. *Endocrinology*. 2004;**145**:113–125.
17. Papapetropoulos A, Pyriochou A, Altaany Z, Yang G, Marazioti A, Zhou Z, Jeschke MG, Branski LK, Herndon DN, Wang R, Szabo C. Hydrogen sulfide is an endogenous stimulator of angiogenesis. *Proc Natl Acad Sci USA*. 2009;**106**:21972–21977.
18. Ribatti D, Nico B, Vacca A, Roncali L, Dammacco F. Endothelial cell heterogeneity and organ specificity. *J Hematother Stem Cell Res*. 2002;**11**:81–90.
19. Bird IM, Sullivan JA, Di T, Cale JM, Zhang L, Zheng J, Magness RR. Pregnancy-dependent changes in cell signaling underlie changes in differential control of vasodilator production in uterine artery endothelial cells. *Endocrinology*. 2000;**141**:1107–1117.
20. Hackam DG, Redelmeier DA. Translation of research evidence from animals to humans. *JAMA*. 2006;**296**:1727–1732.
21. Kho D, MacDonald C, Johnson R, Unsworth CP, O'Carroll SJ, du Mez E, Angel CE, Graham ES. Application of xCELLigence RTCA biosensor technology for revealing the profile and window of drug responsiveness in real time. *Biosensors (Basel)*. 2015;**5**:199–222.
22. Liao WX, Feng L, Zhang H, Zheng J, Moore TR, Chen DB. Compartmentalizing VEGF-induced ERK2/1 signaling in placental artery endothelial cell caveolae: a paradoxical role of caveolin-1 in placental angiogenesis in vitro. *Mol Endocrinol*. 2009;**23**:1428–1444.
23. Zhang HH, Lechuga TJ, Tith T, Wang W, Wing DA, Chen DB. S-nitrosylation of cofilin-1 mediates estradiol-17beta-stimulated endothelial cytoskeleton remodeling. *Mol Endocrinol*. 2015;**29**:434–444.
24. Jaffe EA, Nachman RL, Becker CG, Minick CR. Culture of human endothelial cells derived from umbilical veins: identification by morphologic and immunologic criteria. *J Clin Invest*. 1973;**52**:2745–2756.
25. Hoeben A, Landuyt B, Highley MS, Wildiers H, Van Oosterom AT, De Bruijn EA. Vascular endothelial growth factor and angiogenesis. *Pharmacol Rev*. 2004;**56**:549–580.
26. Orlidge A, D'Amore PA. Inhibition of capillary endothelial cell growth by pericytes and smooth muscle cells. *J Cell Biol*. 1987;**105**:1455–1462.
27. Yan Q, Vernon RB, Hendrickson AE, Sage EH. Primary culture and characterization of microvascular endothelial cells from Macaca monkey retina. *Invest Ophthalmol Vis Sci*. 1996;**37**:2185–2194.

28. Craig LE, Spelman JP, Strandberg JD, Zink MC. Endothelial cells from diverse tissues exhibit differences in growth and morphology. *Microvasc Res*. 1998;**55**:65–76.
29. Thorin E, Shreeve SM. Heterogeneity of vascular endothelial cells in normal and disease states. *Pharmacol Ther*. 1998;**78**:155–166.
30. Hewett PW, Murray JC. Human omental mesothelial cells: a simple method for isolation and discrimination from endothelial cells. *In Vitro Cell Dev Biol Anim*. 1994;**30**:145–147.
31. Plendl J, Neumuller C, Vollmar A, Auerbach R, Sinowatz F. Isolation and characterization of endothelial cells from different organs of fetal pigs. *Anat Embryol (Berl)*. 1996;**194**:445–456.
32. Govers R, Rabelink TJ. Cellular regulation of endothelial nitric oxide synthase. *Am J Physiol Renal Physiol*. 2001;**280**:F193–F206.
33. Liao WX, Feng L, Zheng J, Chen DB. Deciphering mechanisms controlling placental artery endothelial cell migration stimulated by vascular endothelial growth factor. *Endocrinology*. 2010;**151**:3432–3444.
34. Itoh S, Brawley L, Wheeler T, Anthony FW, Poston L, Hanson MA. Vasodilation to vascular endothelial growth factor in the uterine artery of the pregnant rat is blunted by low dietary protein intake. *Pediatr Res*. 2002;**51**:485–491.
35. Wang R. Physiological implications of hydrogen sulfide: a whiff exploration that blossomed. *Physiol Rev*. 2012;**92**: 791–896.
36. Zhao W, Zhang J, Lu Y, Wang R. The vasorelaxant effect of H(2)S as a novel endogenous gaseous K(ATP) channel opener. *EMBO J*. 2001;**20**:6008–6016.
37. Li Y, Zang Y, Fu S, Zhang H, Gao L, Li J. H2S relaxes vas deferens smooth muscle by modulating the large conductance Ca2 +-activated K+ (BKCa) channels via a redox mechanism. *J Sex Med*. 2012;**9**:2806–2813.
38. Yang G, Wu L, Jiang B, Yang W, Qi J, Cao K, Meng Q, Mustafa AK, Mu W, Zhang S, Snyder SH, Wang R. H2S as a physiologic vasorelaxant: hypertension in mice with deletion of cystathionine gamma-lyase. *Science*. 2008;**322**:587–590.
39. Wang K, Ahmad S, Cai M, Rennie J, Fujisawa T, Crispi F, Baily J, Miller MR, Cudmore M, Hadoke PW, Wang R, Gratacos E, Buhimschi IA, Buhimschi CS, Ahmed A. Dysregulation of hydrogen sulfide producing enzyme cystathionine gamma-lyase contributes to maternal hypertension and placental abnormalities in preeclampsia. *Circulation*. 2013;**127**:2514–2522.